JOURNAL OF BACTERIOLOGY, Dec. 2011, p. 6586–6596 Vol. 193, No. 23
0021-9193/11/$12.00 doi:10.1128/JB.05790-11

Characterization of the *mmsAB-araD1* (*gguABC*) Genes of *Agrobacterium tumefaciens*▽

Jinlei Zhao and Andrew N. Binns*

Department of Biology, University of Pennsylvania, 415 South University Ave., Philadelphia, Pennsylvania 19104-6018

Received 13 July 2011/Accepted 26 September 2011

The *chvE-gguABC* operon plays a critical role in both virulence and sugar utilization through the activities of the periplasmic ChvE protein, which binds to a variety of sugars. The roles of the GguA, GguB, and GguC are not known. While GguA and GguB are homologous to bacterial ABC transporters, earlier genetic analysis indicated that they were not necessary for utilization of sugars as the sole carbon source. To further examine this issue, in-frame deletions were constructed separately for each of the three genes. Our growth analysis clearly indicated that GguA and GguB play a role in sugar utilization and strongly suggests that GguAB constitute an ABC transporter with a wide range of substrates, including L-arabinose, D-fucose, D-galactose, D-glucose, and D-xylose. Site-directed mutagenesis showed that a Walker A motif was vital to the function of GguA. We therefore propose renaming *gguAB* as *mmsAB*, for multiple monosaccharide transport. A *gguC* deletion affected growth only on L-arabinose medium, suggesting that *gguC* encodes an enzyme specific to L-arabinose metabolism, and this gene was renamed *araD1*. Results from bioinformatics and experimental analyses indicate that *Agrobacterium tumefaciens* uses a pathway involving nonphosphorylated intermediates to catabolize L-arabinose via an L-arabinose dehydrogenase, $AraA_{At}$, encoded at the Atu1113 locus.

The soilborne bacterium *Agrobacterium tumefaciens* is a Gram-negative plant pathogen that is found in a wide range of environments around the world (for a review, see reference 8). In its saprophytic state, *Agrobacterium* depends on—and competes for—a wide variety of sugars as well as other nutrients that may be available in the soil. In this report, we present experiments that help us understand the role played by the *chvE-gguABC* operon in such processes. Specifically, the activities of mutants deficient in *gguA*, *gguB*, and *gguC* support the hypothesis that the first two of these genes encode proteins involved in sugar uptake, while the GguC protein is involved in an arabinose metabolic pathway that also involves the activity of an arabinose dehydrogenase encoded at gene locus Atu1113.

Consistent with its occurrence in an environment that often results in a paucity of nutrients, *A. tumefaciens* appears to have evolved a variety of high-affinity uptake systems for the acquisition of nutrients. The genome sequence of *A. tumefaciens* indicates that it has 153 complete ATP-binding cassette (ABC) transport systems plus additional "orphan" subunits, which account for 60% of its total transporter complement (35). This compares with 57 ABC transporters in *Escherichia coli* (20). ABC transporters are used by organisms to transport substrates from the surrounding environment into cytoplasm, and they exist widely in organisms from bacteria to humans and have a broad range of substrates (for reviews, see references 15 and 26). In terms of structure, ABC transporters consist of two nucleotide-binding domains (NBDs) and two transmembrane domains (TMDs). These domains can be individual proteins or separate domains in one protein. The NBDs are involved in binding and hydrolysis of ATP, and they are highly conserved at the primary sequence level. Based on sequence and function, NBDs can be divided into three short sequence motifs: Walker A, Walker B, and the signature motif containing the sequence LSGGQ (26).

In *A. tumefaciens* the *chvE*-, *gguA*-, and *gguB*-encoded products are predicted to constitute a complete binding-protein-dependent ABC transporter. ChvE is a periplasmic sugar-binding protein homologous to the sugar-binding proteins involved in ABC transporter systems of numerous well-characterized sugar uptake systems (14). Besides its role in sugar utilization, ChvE also plays a role in the control of virulence (*vir*) gene expression from the tumor-inducing (Ti) plasmid. This occurs via a proposed interaction between ChvE and the periplasmic domain of the histidine kinase, VirA, resulting in increased sensitivity of that protein for inducing phenolics as well as causing an increase in maximal levels of *vir* gene expression at saturating levels of the phenolics (for a review, see reference 21). GguA and GguB are predicted to be an ATP-binding protein and a transmembrane protein, respectively. They belong to the carbohydrate uptake transporter 2 (CUT2) family, which transports only monosaccharides (28). Unlike classic ABC transporters, the integral membrane protein in the CUT2 family contains more transmembrane segments (usually at least 10), and the ATPase protein has two NBDs, in which arginine replaces lysine in the Walker A motif of the C-terminal NBD (28). Like AraG/RbsA family members (28), GguA contains two NBDs. Like most of the transmembrane components in the CUT2 family, GguB is predicted to contain 11 transmembrane domains (http://www.cbs.dtu.dk/services/TMHMM/). GguC, the last gene product encoded by the *chvE-gguABC* operon, has an as-yet-uncharacterized function.

Kemner et al. reported that insertion mutations in *gguA*, *gguB*, or *gguC* did not affect growth of *A. tumefaciens* in the presence of sugars such as galactose, glucose, and arabinose

* Corresponding author. Mailing address: Department of Biology, University of Pennsylvania, 415 South University Ave., Philadelphia, PA 19104-6018. Phone: (215) 898-8684. Fax: (215) 898-8780. E-mail: abinns@sas.upenn.edu.

▽ Published ahead of print on 7 October 2011.

TABLE 1. Strains and plasmids used in this study

Strain or plasmid	Characteristics	Reference or source
E. coli XL1-Blue	*recA1 endA1 gyrA96 thi-1 hsdR17 supE44 relA1 lac*[F′ *proAB lacI*^{q}*Z*ΔM15 Tn*10* (Tc^r)]	Stratagene
A. tumefaciens strains		
A348	C58 background carrying pTiA6	13
AB510	A348, *gguA* deletion	This study
AB520	A348, *gguB* deletion	This study
AB530	A348, *gguC* deletion	This study
AB540	A348, *gguAB* deletion	This study
AB533	A348, but with RGS-6His-tagged *gguC*	This study
AB600	A348, with gene locus Atu1113 deletion	This study
AB601	A348 but with RGS-6His tag at the N terminus of the Atu1113-encoded protein	This study
AB511	A348, *gguA* and *gbpR* deletion	This study
Plasmids		
pYW15b	Broad-host-range expression vector, P_{N25}-MCS-STOP, IncW, and pBR322ori, Amp^r	30
pBBR1MCS-5	Broad-host-range plasmid cloning vector; Gm^r	18
pK18*mobsacB*	Suicide plasmid in *Xanthomonas campestris* pv. campestris; Km^r	27
pJZ10	*gguA* deletion plasmid in pK18*mobsacB*	This study
pJZ11	*gguB* deletion plasmid in pK18*mobsacB*	This study
pJZ12	*gguC* deletion plasmid in pK18*mobsacB*	This study
pJZ13	*gguAB* deletion plasmid in pK18*mobsacB*	This study
pJZ14	Gene locus Atu1113 deletion plasmid in pK18*mobsacB*	This study
pJZ15	RGS-6His-tagged *gguC* recombination plasmid in pK18*mobsacB*	This study
pJZ16	P_{N25}-*gguC* in pYW15b	This study
pJZ17	P_{N25}-Atu1113 in pYW15b	This study
pJZ18	pBBR1MCS-5+P2+*gguA*	This study
pJZ19	pBBR1MCS-5+P2+*gguB*	This study
pJZ20	pBBR1MCS-5+P2+*gguA*-His	This study
pJZ21	pBBR1MCS-5+P2+*gguA*(K44A)-His	This study
pJZ22	RGS-6His-tagged gene locus Atu1113 recombination plasmid in pK18*mobsacB*	This study

(17). However, our recent studies clearly indicate that ChvE can bind numerous different monosaccharides and is important in sugar utilization (14). Given that their amino acid sequences suggest that GguA and GguB are typical of sugar transporters, we sought to unravel this conflict and better understand the role of the *chvE-gguABC* operon in sugar utilization. Toward this end, we generated strains with deletions of *gguA*, *gguB*, or *gguC* and characterized their growth in medium containing various sugars. The data presented here indicate that GguA and GguB are, in fact, involved in the utilization of multiple sugars. Moreover, site-directed mutagenesis confirmed the importance of the putative ATP binding site of GguA. Therefore, we propose renaming *gguAB* as *mmsAB*, for multiple monosaccharide transport. Growth analysis also indicated that *gguC* is involved in arabinose utilization but not utilization of other sugars. Further investigation indicates that in *A. tumefaciens*, L-arabinose is catabolized by a pathway involving nonphosphorylated intermediates via an arabinose dehydrogenase encoded at gene locus Atu1113 on the chromosome of *A. tumefaciens* A348. In keeping with nomenclature of the gene in *Azospirillum brasiliense* (33), we name the gene at locus Atu1113 $araA_{At}$.

MATERIALS AND METHODS

Bacterial growth assays. *A. tumefaciens* strains (Table 1) were first grown in Luria-Bertani (LB) medium (22) at 25°C. After 20 h of growth, the cultures were spun down, resuspended, and diluted to an optical density at 600 nm (OD_{600}) of 0.1 in AB minimal medium (5) with 10 mM glycerol (Invitrogen) as the sole carbon source. The cultures were grown for another 20 h and then diluted to an OD_{600} of 0.06 in AB minimal medium in the presence of different sugars as the sole carbon source. The carbon sources, L-arabinose (Sigma), D-fucose (Sigma), D-galactose (Fisher Scientific), D-glucose (Fisher Scientific), glycerol, and D-xylose (Sigma), were used at 3 mM. Cultures were incubated with shaking at 25°C at 200 rpm. At intervals, OD_{600} measurements were taken with a spectrophotometer (Beckman DU 520). No growth was observed when the strains checked were incubated in minimal medium without a carbon source.

Deletion strain construction. We used marker exchange eviction mutagenesis (27) to create strains carrying nonpolar deletions of *gguA*, *gguB*, *gguAB*, *gguC*, *gguA* plus *gbpR*, and the Atu1113 locus in the chromosome of A348 (13). Construction of these deletions used sequential-pair PCRs (16) and the suicide plasmid pK18*mobsacB* (27). For the *gguA* mutation, a 4-nucleotide (nt) overlap region between the stop codon of *gguA* and the start codon of *gguB* (Fig. 1) necessitated retaining the 3′ end of *gguA* in order to keep the start codon and ribosome binding site of *gguB* intact and allow expression of *gguB*. Primer P4, located 71 nt upstream from the start codon of *gguB* (within *gguA*), was used with P3 (located within *gguB*) to amplify a 675-bp fragment containing the downstream *gguA*-flanking sequence and the 3′ end of *gguA*. PCR to amplify the upstream *gguA*-flanking sequence used primers P1 and P2 to create a 600-bp product that included promoter P2. The 5′ ends of primers P4 and P1 had been designed to include complementary sequence so that the products from the first two PCRs could function as self-annealing templates in a third PCR with primers

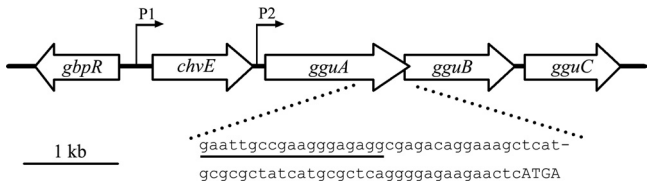

FIG. 1. Gene map of the *chvE-gguABC* region of *A. tumefaciens* A348. The positions of promoters P1 and P2 are indicated. Arrows indicate the direction in which the genes are expressed. The enlarged region shows the 4-nt overlap sequence (uppercase) of start codon of *gguB* (ATG) and stop codon of *gguA* (TGA) and the position of *gguA* deletion primer P4 (underlined sequence).

TABLE 2. Primers used in this study

Primer	Sequence (5′ to 3′)[a]	Description
P1	TCGGCAATTCATCGCAATCCAGCGCCCG	Deletion of *gguA*
P2	ACA**GAATTC**GACAGCGGCAAGCTGGTC	Deletion of *gguA*
P3	GAGTAC**AAGCTT**CCAGATAGAACAGCGCGAC	Deletion of *gguA*
P4	GGATTGCGATGAATTGCCGAAGGGAGAGG	Deletion of *gguA*
P5	ACTG**TCTAGA**TCAAGGTTGTTCCGTCCTAC	Construction of *gguA* and *gguB* complementation
P6	TCA**GGTACC**TCATGCCGAACTCATGAGTTCTTC	Construction of *gguA* complementation
P7	GAGTAC**AAGCTT**ACGGAGAGGTGAGAGCCG	Deletion of *gguB*
P8	CATGAGTTGATCGGCCCAACTCCTAT	Deletion of *gguB*
P9	GGGCCGATCAACTCATGAGTTCTTCTCCC	Deletion of *gguB*
P10	ACA**GAATTC**CAAGTCCTATGGCCACAGG	Deletion of *gguB*
P12	TGATAGCGCGCATCGCCCGATTAATTCAGACG	Construction of *gguB* complementation
P13	TCA**GGTACC**TTGACTGCGATAGGAGTTGG	Construction of *gguB* complementation
P14	AATTAATCGGGCGATGCGCGCTATCATGCGCT	Construction of *gguB* complementation
P15	ACT**GGATCC**CATCCGCCATTATGGAAACC	Deletion of *gguC*
P16	GCAGGTGCATCTGACGGACTGCGTATGA	Deletion of *gguC*
P17	TCCGTCAGATGCACCTGCATCTTATGAAAG	Deletion of *gguC*
P18	ACA**CTGCAG**CATCGTGCAGAATCTGCTGA	Deletion of *gguC*
P19	ACT**GAGCTC**ATGCACCGCGTAGAAGAGA	Construction of *gguC* complementation
P20	TCAG**AAGCTT**TCAGATCTGCCGAACCACG	Construction of *gguC* complementation
P21	ACTG**TCTAGA**TCAAGGTTGTTCCGTCCTAC	Construction of *gguA*(K44A)-His complementation
P22	GCGGGGGCCTCGACCTTGATGAAGGTCCT	Construction of *gguA*(K44A)-His complementation
P23	CAAGGTCGAGGCCCCCGCGCCGTTCTCAC	Construction of *gguA*(K44A)-His complementation
P24[b]	TCA**GGTACC**TTAGTGATGGTGATGGTGATGTGAGTTCTTCTCCCCTGAGC	Construction of *gguA*(K44A)-His complementation
P25[c]	GGTGCAATGAGAGGATCGCATCACCATCACCATCACCGCGTAGAAGAGACAAG	RGS-6His-tagged *gguC in situ* replacement
P26	GCGATCCTCTCATTGCACCTGCATCTTATGA	RGS-6His-tagged-*gguC in situ* replacement
P27	GGA**AGATCT**CGGAGCGCTTCTGAGACTG	Deletion of gene locus Atu1113
P28	CCTCTCCATGTGAGAAGCCTCAACGCTTCC	Deletion of gene locus Atu1113
P29	AGGCTTCTCACATGGAGAGGGATCCGTTTG	Deletion of gene locus Atu1113
P30	GAGTAC**AAGCTT**CCGGACGTCATCGAAAGC	Deletion of gene locus Atu1113
P31	ACT**GAGCTC**ATGTCAGCCACCAAGCTTGC	Construction of gene locus Atu1113 complementation
P32	ACGCT**GTCGAC**TCAGTCGTAGAACGAATCCAC	Construction of gene locus Atu1113 complementation
P33[d]	CGCGGCTCGCATCACCATCACCATCACTCAGCCACCAAGCTTGCCA	RGS-6His-tagged gene locus Atu1113 *in situ* replacement
P34	ATGGTGATGCGAGCCGCGCATGGAGAGGGATCCGTTTG	RGS-6His-tagged gene locus Atu1113 *in situ* replacement
P35	CGG**CTCGAG**CCGGACGTCATCGAAAGC	RGS-6His-tagged gene locus Atu1113 *in situ* replacement
P36	GAGTAC**AAGCTT**GATCTGGGACAGCTGGTTC	Deletion of *gbpR*
P37	TTGGTCAGCTCATGCGCAGGTGGCTCAT	Deletion of *gbpR*
P38	CTGCGCATGAGCTGACCAACACCTGACG	Deletion of *gbpR*
P39	ACA**GAATTC**CGTTTTCAGCGGAAATGCT	Deletion of *gbpR*
P40	GGATTGCGATTCGGCCCAACTCCTATCG	Deletion of *gguAB*
P41	TTGGGCCGAATCGCAATCCAGCGCCCG	Deletion of *gguAB*

[a] Boldface type indicates engineered restriction sites.
[b] Underlining indicates the added 6-His tag before the stop codon of *gguA*.
[c] Underlining indicates the added RGS-6His tag after the start codon of *gguC*.
[d] Underlining indicates the added RGS-6His tag after the start codon of the protein encoded by the gene locus Atu1113.

P3 and P4 to generate a 1.3-kb fragment carrying *gguA*-flanking sequences and a small segment at the 3′ end of *gguA*. This 1.3-kb PCR fragment was digested with HindIII and EcoRI and cloned into pK18*mobsacB*. The resulting construct pJZ10 was electroporated into A348. Colonies which underwent an initial recombination event were identified by their ability to grow on LB medium with kanamycin. Cells which underwent a second recombination, which is predicted to remove all vector sequences, were identified by growth on LB medium with 10% sucrose. A resulting isolate, containing the putative nonpolar *gguA* null mutation, was confirmed with PCR using primers that were (i) outside the region of exchange, which yielded a smaller PCR product than PCR with the wild type as the template, and (ii) internal to the *gguA* region, which yielded no PCR product. This *gguA*-null mutant was named AB510.

Similar strategies were used to construct the *gguB*, *gguC*, *gguAB*, *gguA* plus *gbpR*, and gene locus Atu1113 nonpolar deletion strains AB520, AB530, AB540, AB511, and AB600, respectively. The primers used in these strain constructions are shown in Table 2. For the *gguB* deletion, downstream and upstream *gguB*-flanking sequences were amplified using primer pairs P7-P8 and P9-P10, respectively. Note that an additional TCA sequence was added before the *gguA-gguB* overlap sequence ACTCAT in primer P9 to keep the stop codon of *gguA* intact. The third PCR was conducted using primers P7 and P10 with the two PCR

products from the first PCRs as the template. For the *gguC* deletion, primer pairs P15-P16 and P17-P18 were used to amplify downstream and upstream *gguC*-flanking sequences, respectively. Primers P15 and P18 were further used for the third PCR. For the *gguAB* deletion, downstream and upstream *gguAB*-flanking sequences were amplified using primer pairs P7-P40 and P41-P2, respectively. The third PCR was conducted using primers P7 and P2 with the two PCR products from the first PCRs as the template. For the deletion of the gene at locus Atu1113, primer pairs P27-P28 and P29-P30 were used to amplify downstream and upstream Atu1113-flanking sequences, respectively. In the third PCR, primers P27 and P30 were used. The *gbpR* deletion was created in the AB510 (Δ*gguA*) background. Primer pairs P36-P37, P38-P39 were used to amplify downstream and upstream *gbpR*-flanking sequences, respectively. Primers P36 and P39 were further used in the third PCR. The final PCR products were cloned into pK18*mobsacB* separately and transferred into *Agrobacterium* for homologous recombination. All mutant strains thus obtained were confirmed by the PCR strategy described above for AB510.

Constructions of plasmids used in complementation of the *gguA*, *gguB*, *gguC*, and gene locus Atu1113 deletions. Besides the inducible promoter P1 upstream of *chvE*, a second promoter, P2, which drives transcription of *gguABC*, is located upstream of *gguA* (11, 17). For *gguA* complementation, primers P5 and P6 were used to amplify the *gguA* open reading frame with its promoter, P2. The 1.7-kb PCR fragment was digested with XbaI and KpnI and cloned into pBBR1MCS-5 (18), yielding pJZ18. For *gguB* complementation, primers P5 and P12 were used to amplify a 0.2-kb fragment carrying promoter P2. Primers P13 and P14 were used to amplify the 1.2-kb *gguB* open reading frame. The two PCR products described above were mixed and used as a template for a third PCR with primers P5 and P13 to obtain the *gguB* open reading frame driven by promoter P2. This 1.4-kb product was digested with XbaI and KpnI and cloned into pBBR1MCS-5, yielding pJZ19. For *gguC* complementation, primers P19 and P20 were used to amplify the 1.0-kb *gguC* open reading frame. The PCR product was digested with SacI and HindIII and then cloned into pYW15b, yielding pJZ16, in which *gguC* is driven by the constitutively expressed P_{N25} promoter (30). For gene locus Atu1113 complementation, primers P34 and P35 were used to amplify the 930-bp gene locus Atu1113. The PCR product was digested with SacI and SalI and cloned into pYW15b, yielding pJZ17.

RGS-6His-tagged *gguC* and RGS-6His-tagged gene locus Atu1113 *in situ* replacement. In order to monitor the expression of GguC, we fused an RGS-6His tag to the N terminus of *gguC* and placed it at the original *gguC* location in the chromosome (RGS is arginine-glycine-serine). Two initial PCRs used primer pairs P15-P25 and P18-P26. Subsequently, the products from the first two PCRs were used as templates to create a fragment carrying the RGS-6His-tagged *gguC* gene in addition to 600 bp of upstream and 600 bp of downstream sequences. The latter PCR used primers P15 and P18. The final PCR fragment was digested with BamHI and PstI and was cloned into pK18*mobsacB* to create plasmid pJZ15. The plasmid was introduced into AB530, and transformants were screened as described above. A resulting isolate, containing N-terminal RGS-6His-tagged GguC, was confirmed with PCR using primers that were outside the region of mutagenesis, which yielded a larger PCR product than PCR with AB530 as the template. The sequence authenticity of the N-terminal RGS-6His-tagged GguC of this isolate was further verified by sequencing. The strain was named AB533.

The same method was also used to create an RGS-6His-tagged gene at the Atu1113 chromosomal locus using primers shown in Table 2. The first PCRs were done using primer pairs P27-P28 and P29-P30. Subsequently, primers P27 and P30 were used for overlap PCR with the first two PCR products as the template. The final PCR fragment was cloned into pK18*mobsacB* and subsequently introduced into AB600 for crossover events. The strain thus obtained with the RGS-6His at the N terminus of the protein product encoded by gene locus Atu1113 was named AB601, and it was confirmed by PCR and verified by sequencing as described for AB533.

Site-directed mutation in the ATP-binding site of GguA. Overlap extension PCR was used to generate a mutation (K44A) in the GguA Walker A ATP-binding site. Primers P5 and P22 were used to amplify the promoter P2 of *gguA* and the first 44 codons of *gguA*. Primers P23 and P24 were used to amplify the remainder of *gguA* with the addition of six histidines at the C terminus immediately preceding the stop codon. These two PCR products were mixed and used as the template for the third PCR with primers P5 and P24. The third PCR product was digested by KpnI and XbaI and cloned into pBBR1MCS-5 to make pJZ21. As a control, the wild-type *gguA* was also amplified with primers P5 and P24 and cloned into pBBR1MCS-5 to make pJZ20.

***A. tumefaciens* CFE preparation.** A single colony of the tested strain was inoculated into LB medium and incubated with aeration at 25°C overnight. The cultures were then inoculated (OD_{600} = 0.1) into AB minimal medium with 10 mM L-arabinose. The cultures were grown approximately 20 h and collected for cell-free extract (CFE) preparation. Cell pellets were resuspended in 20 mM phosphate-buffered saline (PBS) (pH 7.0) buffer and subjected to sonication. After centrifugation at 13,000 × *g* for 15 min, the supernatant (CFE) was collected.

L-Arabinose dehydrogenase and L-arabinose isomerase assay. L-Arabinose 1-dehydrogenase activity was assayed routinely in the direction of L-arabinose oxidation by measuring the production of NAD(P)H by monitoring absorbance at 340 nm at 25°C as previously described (31). The standard assay mixture contained 10 mM L-arabinose in 100 mM Tris-HCl (pH 9.0) buffer. The reaction was started by the addition of 10 mM $NAD(P)^+$ solution (100 μl) with a final reaction volume of 1 ml. CFE protein concentrations were determined with the BCA protein assay kit (Pierce), and approximately 100 μg CFE was added to the 1-ml reaction mixture.

L-Arabinose isomerase activity was measured as described by Cribbs and Englesberg (7). CFE (40 μl) was incubated with 60 μl of assay mix (100 mM Tris-HCl [pH 7.5], 100 mM L-arabinose, 1 mM $MnCl_2$) at 25°C for 30 min. The reaction was terminated with the addition of 0.9 ml of 100 mM HCl, and the cysteine-carbazole test was used to measure production of ribulose (10).

Immunoblot analysis of the expression of ChvE, GguC, GguA, GguA(K44A), and the L-arabinose dehydrogenase encoded at gene locus Atu1113. Bacteria were grown in AB medium with various sugars as the sole carbon source. They were collected and adjusted to an OD_{600} of 20. After addition of sample buffer (19), they were boiled for 10 min. Samples (10 μl each) were subjected to sodium dodecyl sulfate-polyacrylamide gel electrophoresis (SDS-PAGE) and subsequently transferred to a polyvinylidene difluoride membrane (Millipore). For immunoblot analysis, penta-His mouse monoclonal antibody (Qiagen) was used to detect 6His-tagged GguA and GguA(K44A), while RGS-His mouse monoclonal antibody (Qiagen) was used to detect the RGS-6His-tagged protein encoded at gene locus Atu1113 and RGS-6His-tagged GguC. Proteins were visualized with horseradish peroxidase-conjugated anti-mouse immunoglobulin secondary antibody (Amersham) and ECL Plus (Amersham). To check the ChvE expression level, anti-ChvE rabbit antibody was used as the primary antibody (14).

RESULTS

***gguA*, *gguB*, and *gguC* mutants are differentially deficient in carbon source utilization.** In-frame deletions in genes downstream from *chvE* (*gguA*, *gguB*, and *gguC*) were used to characterize sugar utilization in *A. tumefaciens*. For this purpose, mutants AB510 (Δ*gguA*), AB520 (Δ*gguB*), and AB530 (Δ*gguC*) were derived from wild-type strain A348. Because there is a 4-nt overlap region between the stop codon of *gguA* and the start codon of *gguB* (17) (Fig. 1), the deletion of *gguA* was constructed so that the start codon and ribosome-binding site of *gguB* remained intact (see Materials and Methods for details). The strains carrying the *gguA*, *gguB*, and *gguC* deletions were tested for growth on various sugars as the sole carbon source. For this purpose, mutant and wild-type (A348) strains were grown in AB medium supplied with either glycerol or one of several sugars (L-arabinose, D-fucose, D-galactose, D-glucose, or D-xylose). All of the mutant strains were able to utilize glycerol and grow as well as the wild-type strain (Fig. 2). Compared to A348, AB510 (Δ*gguA*) and AB520 (Δ*gguB*) grew slowly in each of the different sugar (3 mM)-containing media but reached the same OD_{600} as A348 after extended cultivation. These data are consistent with the idea that GguA and GguB constitute one transporter which can take up multiple monosaccharides, including L-arabinose, D-fucose, D-galactose, D-glucose, and D-xylose. The capacity of the mutant strains to grow on these sugars (albeit slowly) suggests that there is at least one other pathway for transporting these sugars. One unexpected observation was that while the strains carrying the *gguA* and *gguB* deletions exhibited virtually identical growth curves when provided galactose, glucose, or xylose as the sole carbon source,

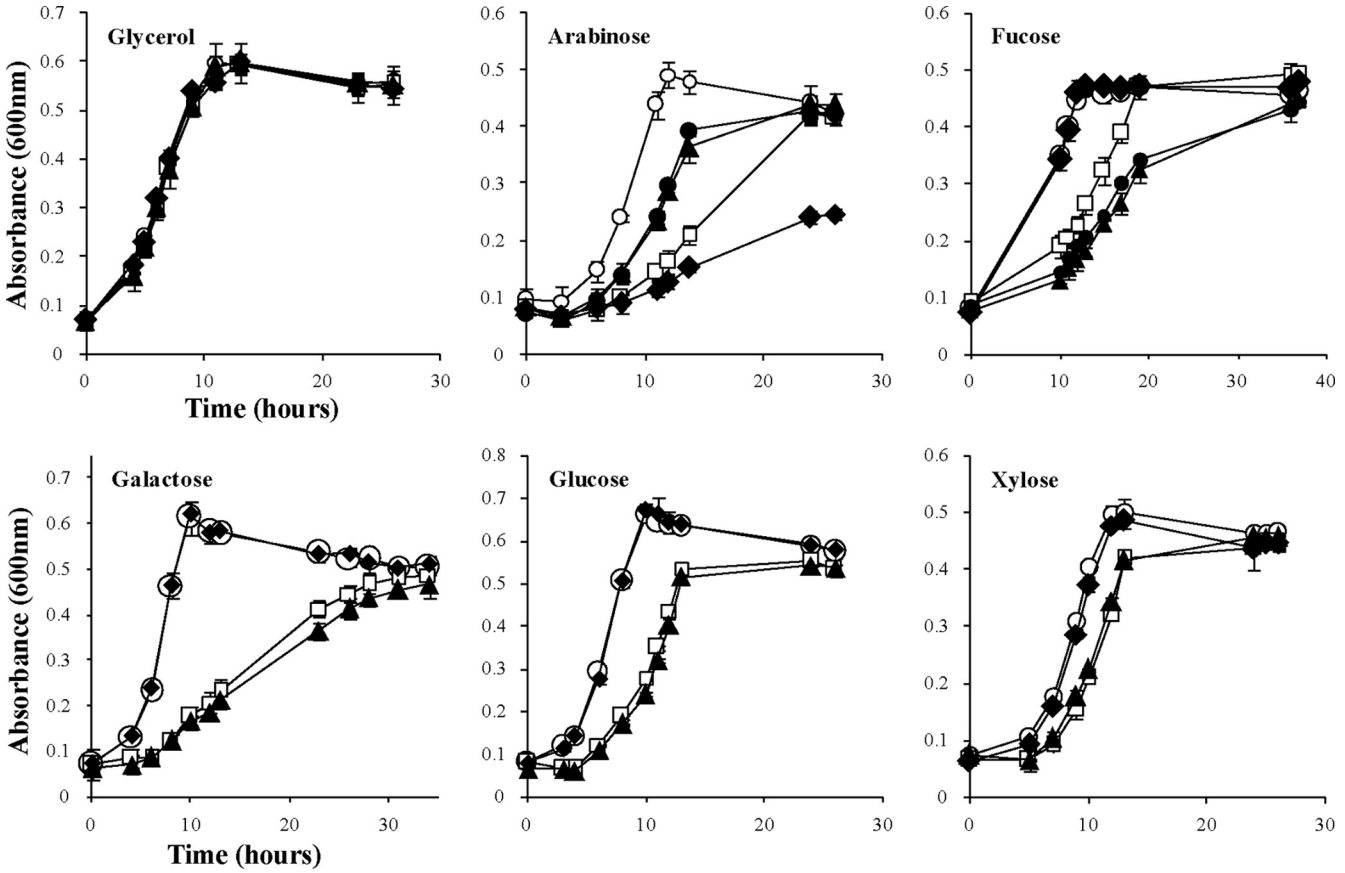

FIG. 2. Growth curves of *A. tumefaciens* wild type and *gguABC* mutants in minimal medium containing different sugars. Bacteria were grown at 25°C in AB minimal medium with 3 mM glycerol or various monosaccharides as the sole carbon source. At intervals, the optical density at 600 nm of the cultures was determined. Strains used were the wild-type A348 (○), the *gguA* mutant AB510 (□), the *gguB* mutant AB520 (▲), the *gguC* mutant AB530 (◆), and the *gguAB* mutant AB540 (●). Note that AB540 was tested only in minimal medium with arabinose and fucose. Data are the averages of triplicate values with standard deviations.

they exhibited different results when grown with arabinose or fucose. Intriguingly, when the double mutant (Δ*gguAB*) strain AB540 was tested for growth with arabinose or fucose, it exhibited the same growth phenotype as AB520 (Δ*gguB*) (Fig. 2). In contrast to the strains with *gguA* and *gguB* deletions, strain AB530 (Δ*gguC*) grew normally with all sugars tested with the sole exception of arabinose (Fig. 2). Not only did AB530 grow more slowly in arabinose, but it was unable to reach the same cell density as wild-type strain A348 even after cultivation was extended to 150 h (data not shown).

Experiments were carried out to determine whether mutant phenotypes conferred by the *gguA*, *gguB*, and *gguC* deletions could be complemented by adding back an intact version of the deleted gene. Interestingly, when the constitutively expressed promoter P_{N25} was used to drive expression of *gguA* or *gguB*, the strains grew very poorly (data not shown). Given that these constructs were on multicopy plasmids, it appears that their overexpression may be toxic. We therefore used the strategy employed in the analysis of *gguA* and *gguB* in *Brucella suis*, which used the P2 promoter of the operon (1). The data indicate that the *gguA* mutant (AB510) was partially complemented in *trans* with plasmid-borne *gguA* (pJZ18), whereas plasmid-borne *gguB* (pJZ19) fully complemented AB520 (Δ*gguB*) (Fig. 3). The partial complementation of the *gguA* deletion on strain AB510 by pJZ18 may be due to the lack of translational coupling between *gguA* and *gguB* that is suggested by the overlapping stop and start codons in the wild-type strain (Fig. 1). Such coupling is a common feature in operons encoding ABC transporters (3, 4, 25). Finally, plasmid pJZ16, in which *gguC* is driven by the constitutively expressed promoter P_{N25}, fully restored growth of the *gguC* deletion mutant strain AB530 in minimal medium containing arabinose (Fig. 3).

K44 is necessary for GguA function. A typical Walker A motif (G^{38}ENGAGKST^{46}) is found in the N-terminal region of GguA, and the conserved lysine residue (codon 44) is important for binding ATP/ADP in other homologs (9). To further investigate the function of GguA, site-directed mutagenesis was employed to change lysine 44 to alanine. In order to compare the expression levels of GguA(K44A) and wild-type GguA, a 6His tag was added to the C terminus of both GguA(K44A) and wild-type GguA. Immunoblot analysis showed that GguA-His and GguA(K44A)-His expressed from the genes driven by the P2 promoter, were equally abundant (Fig. 4A). Growth assays showed that AB510/pJZ20 (6His-tagged wild-type *gguA*) grew similarly to AB510/pJZ18 (wild-type *gguA*) in arabinose medium, suggesting that the 6His tag

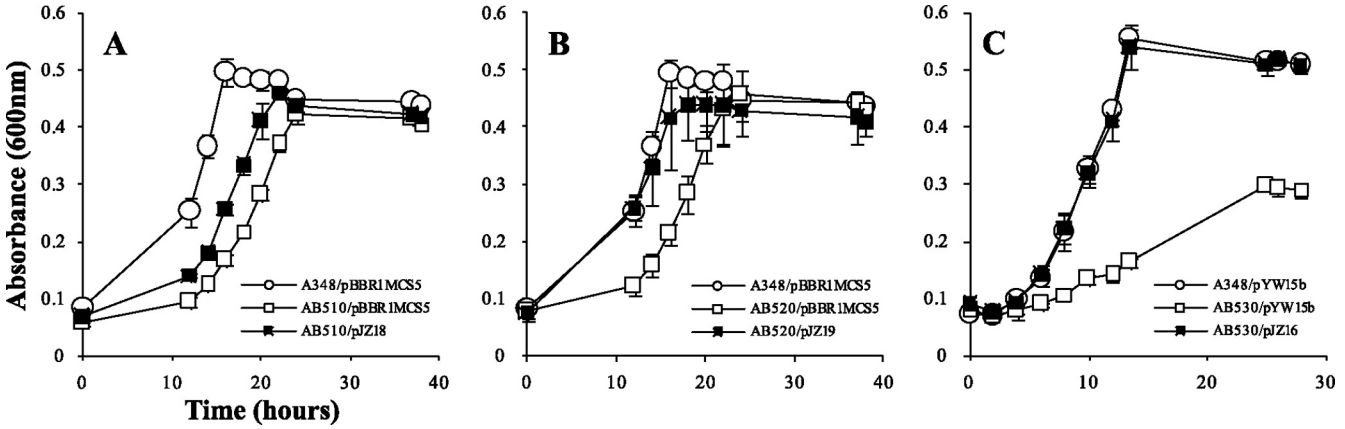

FIG. 3. Growth curves of complementation of *gguABC* mutants in AB minimal medium with 3 mM arabinose. (A) AB510 (*gguA* mutant) and (B) AB520 (*gguB* mutant) were complemented with pBBR1MCS-5 derived plasmids pJZ18 and pJZ19, respectively. (C) AB530 (*gguC* mutant) was complemented with pYW15b based plasmid pJZ16. Data are the averages of triplicate values with standard deviations.

did not affect the function of GguA. In contrast, strain AB510/pJZ21 [*gguA*(*K44A*)-His] demonstrated delayed growth in arabinose, similar to that of AB510 carrying the empty vector (Fig. 4B). These results strongly suggest that the K44 residue is vital for GguA function and that GguA is most likely an ATP-binding protein.

Expression from the P2 promoter is induced by some sugars and regulated by GbpR. The *chvE-gguABC* operon carries two promoters. Expression from the P1 promoter located just 5′ to *chvE* was shown to be inducible by arabinose and galactose, while expression from the P2 promoter between *chvE* and *gguA* was previously suggested to be constitutively expressed and not induced by arabinose or other sugars tested (17). Plasmid pJZ20, carrying *gguA*-His controlled by promoter P2, was used to analyze P2 activity based on the expression of GguA. Immunoblot analysis was used to examine GguA abundance in response to different sugars. Surprisingly, GguA-His was upregulated in the presence of arabinose, fucose, and galactose (Fig. 5A). Doty et al. demonstrated that the arabinose-inducible promoter P1 is regulated by GbpR, a LysR-type regulator (11). The *gbpR* locus is adjacent to *chvE* but divergently transcribed. To determine whether expression from P2 is also regulated by GbpR, we constructed the *gbpR* and *gguA* double-deletion strain AB511. Plasmid pJZ20, harboring *gguA*-His, was introduced into this strain, and immunoblot analysis was used to detect GguA. In the absence of GbpR, GguA, like ChvE, was not subject to regulation by carbon source (Fig. 5B). These results strongly suggest that GbpR regulates promoter P2 as well as promoter P1.

As the growth assay presented in Fig. 2 shows, AB530 demonstrated defective growth only in media containing L-arabinose. We wished to determine whether *gguC* expression is also only induced by L-arabinose. To do this, we added an RGS-6His tag to the N terminus of *gguC* via double crossover as described in Materials and Methods. GguC was upregulated in minimal medium not only with arabinose but also with fucose

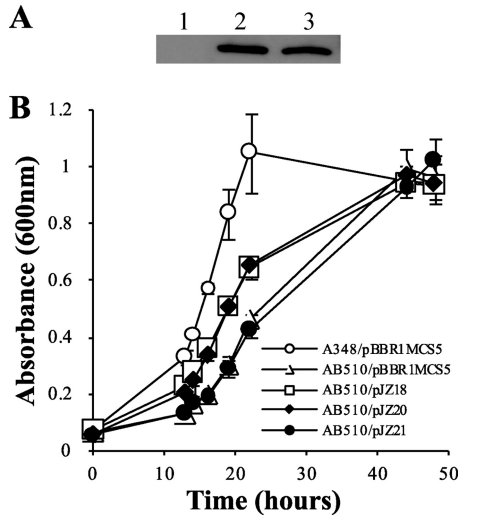

FIG. 4. Effect of the K44A mutation of GguA on protein expression and strain growth ability. (A) Expression level of GguA in the *gguA* deletion strain AB510 carrying 6His-tagged wild-type *gguA* (pJZ20, lane 2), 6His-tagged K44A *gguA* mutant (pJZ21, lane 3), or vector control (pBBR1MCS-5, lane 1). (B) Growth curves of *gguA* mutant AB510 carrying wild-type *gguA* (pJZ18), 6His-tagged wild-type *gguA* (pJZ20), 6His-tagged K44A *gguA* mutant (pJZ21), or vector control (pBBR1MCS-5). The strains were grown in minimal medium containing 10 mM arabinose. Data are the averages of triplicate values with standard deviations.

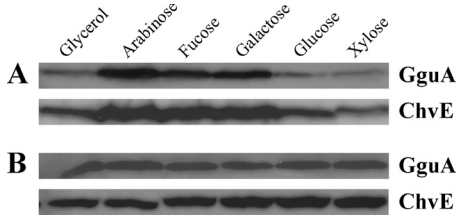

FIG. 5. GguA and ChvE expression in minimal medium containing 10 mM glycerol, arabinose, fucose, galactose, glucose, or xylose as the sole carbon source. The *gguA* deletion strain AB510 (A) or the *gguA* and *gbpR* deletion strain AB511 (B) carrying 6His-tagged wild-type *gguA* in pJZ21 was grown in minimal medium with the indicated sugars. After GguA was detected with mouse anti-penta-His antibody, the membrane was stripped and subsequently used to determine the ChvE level with rabbit anti-ChvE antibody.

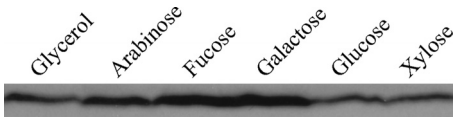

FIG. 6. GguC expression is induced by arabinose, galactose, and fucose. Strain AB533 with RGS-6His-tagged *gguC* was grown in minimal medium containing 10 mM glycerol, arabinose, fucose, galactose, glucose, or xylose as the sole carbon source. After 24 h cultivation, cells were spun down and adjusted to an OD of 20 in PBS buffer. Ten-microliter samples were loaded in each lane. GguC was detected with mouse anti-RGS-His antibody.

and galactose (Fig. 6). This is consistent with the result obtained by Kemner et al. showing that P1 is the primary promoter of *chvE-gguABC* operon and is upregulated in the presence of arabinose, fucose, and galactose. It is also consistent with the result described above showing that P2 is also induced by these sugars.

L-Arabinose degradation in *A. tumefaciens* occurs via a pathway lacking phosphorylated intermediates. The sequence of GguC indicates that it has a fumarylacetoacetase (FAA) hydrolase domain at the C terminus (Pfam [http://pfam.sanger.ac.uk/]). A BLAST search also indicated that GguC is homologous to KdaD (2-keto-3-deoxy-D-arabinonate dehydratase), an enzyme involved in D-arabinose metabolism in *Sulfolobus solfataricus* (see Discussion). This, together with the observed growth defect of AB530 on L-arabinose medium, suggests that GguC is an enzyme involved in L-arabinose metabolism. In bacteria, there are two known pathways for L-arabinose metabolism. One pathway, consisting of phosphorylated intermediates, has been extensively studied. In many bacteria, including *E. coli*, L-arabinose isomerase, ribulokinase, and L-ribulose-phosphate 4-epimerase convert L-arabinose into D-xylulose-5-phosphate (23) (Fig. 7A). The second pathway (Fig. 7B), involving nonphosphorylated intermediates, utilizes L-arabinose 1-dehydrogenase, L-arabinonolactonase, and L-arabonate dehydratase to convert L-arabinose to L-2-keto-3-deoxyarabonate (L-KDA). Metabolism of L-KDA can follow two possible pathways. First, it may be converted into α-ketoglutarate via L-KDA dehydratase and α-ketoglutaric semialdehyde dehydrogenase, as in *Azospirillum brasiliense* (31–33). Alternatively, L-KDA aldolase can convert L-KDA into pyruvate and glycolaldehyde. A BLAST search did not identify homologs to *E. coli* genes involved in L-arabinose metabolism in the *A. tumefaciens* genome. However, several genes homologous to these involved in the alternative pathway found in *A. brasiliense* were found in the genome of *A. tumefaciens* (Table 3). Significantly, the product encoded by the gene locus Atu1113 has 58% identity to AraA (L-arabinose 1-dehydrogenase) in *A. brasiliense* (31). Furthermore, the residues D168 and N172, which are important for catalytic function in L-arabinose 1-dehydrogenase in *A. brasiliense*, were also found in the protein encoded by gene locus Atu1113. This suggests that *A. tumefaciens* degrades L-arabinose in a pathway involving nonphosphorylated intermediates.

To test the hypothesis that *A. tumefaciens* uses such a pathway to metabolize L-arabinose, we first looked for evidence of the enzyme activities that represent the first steps of these two different pathways, L-arabinose isomerase and L-arabinose 1-dehydrogenase. NAD^+- and $NADP^+$-dependent L-arabinose 1-dehydrogenase enzyme activity (138.50 ± 4.02 and 80.64 ± 3.31 nmol min^{-1} mg^{-1}, respectively) was found in cell extracts of *A. tumefaciens* cells grown in AB medium with L-arabinose as the sole carbon source. In contrast, no L-arabinose isomerase activity was observed in *A. tumefaciens*, though the activity was readily observed in cell extracts from *E. coli* (data not shown). This result indicates that *A. tumefaciens* uses a pathway including nonphosphorylated intermediates to metabolize L-arabinose, starting with the enzyme L-arabinose dehydrogenase.

As noted above, the Atu1113 locus is homologous to *araA*, the gene encoding L-arabinose dehydrogenase, in *A. brasiliense*. We constructed AB600, which carries a deletion of the Atu1113 locus, and measured its growth in minimal medium with different sugars. AB600 did not grow with L-arabinose as the sole carbon source (Fig. 8), further supporting the suggestion that the gene at this locus is involved in L-arabinose degradation and that *A. tumefaciens* uses the nonphosphorylation pathway. For consistency and clarification, the Atu1113 locus was named $araA_{At}$. Unexpectedly, AB600 also grew poorly on D-galactose and very poorly on D-fucose (Fig. 8). However, the strain grew normally on galactose, glucose, and xylose. This indicates that $AraA_{At}$ is also involved in D-fucose and D-galactose metabolism. The growth defect of AB600 was successfully complemented with plasmid pJZ17 (Fig. 8). Enzyme assays with overexpressed and purified $AraA_{At}$ further confirmed

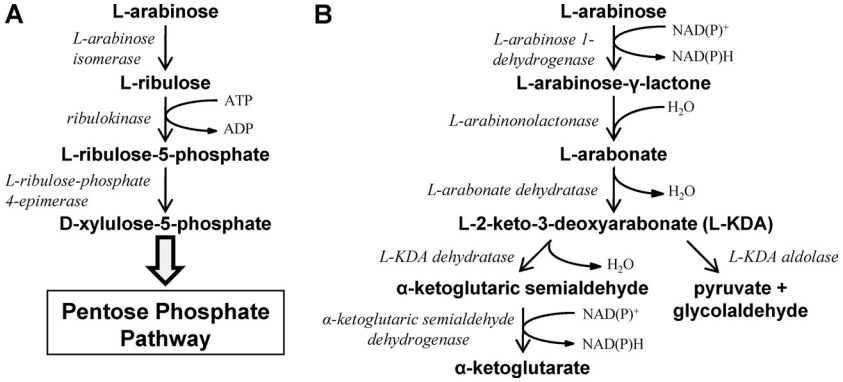

FIG. 7. Pathways of L-arabinose metabolism in bacteria. (A) The well-characterized and long-established phosphorylative pathway in *E. coli* and many other bacteria. The product D-xylulose-5-phosphate is further catabolized via the pentose phosphate pathway. (B) The nonphosphorylative pathway operative in *A. brasiliense* (first pathway) and in several other bacteria (second pathway).

TABLE 3. Genes in *A. tumefaciens* homologous to those involved in L-arabinose metabolism in *A. brasiliense*

ORF in *A. brasiliense* (enzyme name; length[a])	Homolog in *A. tumefaciens*[b]	Length[a]	Expect value	% Identity/ range[d]	Annotation
araA (L-arabinose 1-dehydrogenase; 309)	Atu1113	308	2e-93	58/303	Dehydrogenase
	Atu5435	390	1e-07	33/132	Oxidoreductase
	Atu3347	377	2e-07	24/251	Hypothetical protein
araB (L-arabinolactonase; 300)	Atu5464	560	6e-29	35/283	IclR family transcriptional regulator
	Atu0702	295	9e-26	34/274	Calcium-binding protein, regucalcin
	Atu4190	293	1e-20	30/256	Calcium-binding protein, regucalcin
	Atu3962	269	1e-20	29/272	Calcium-binding protein, regucalcin
	Atu4029	306	3e-08	31/145	Gluconolactonase precursor
araC (L-arabonate dehydratase; 593)	Atu3971	574	3e-136	47/568	Dihydroxy-acid dehydratase
	Atu3219	603	1e-114	46/543	Dihydroxy-acid dehydratase
	Atu2736	594	3e-103	41/593	Dihydroxy-acid dehydratase
	Atu1918	611	8e-56	33/584	Dihydroxy-acid dehydratase
	Atu0598	606	1e-33	27/518	Phosphogluconate dehydratase
araD (L-2-keto-3-deoxyarabonate dehydratase; 309)	Atu5457	302	7e-20	31/286	Dihydrodipicolinate synthase
	Atu1024	294	4e-11	27/137	Dihydrodipicolinate synthase
araE (α-ketoglutaric semialdehyde dehydrogenase; 481)[c]	Atu3498	478	2e-175	63/476	Aldehyde dehydrogenase
	Atu4247	484	2e-90	41/466	Aldehyde dehydrogenase
	Atu3403	485	2e-86	41/467	Succinate semialdehyde dehydrogenase
	Atu5137	484	6e-84	39/477	NAD-dependent succinyl-semialdehyde dehydrogenase
	Atu4762	492	6e-78	39/466	Succinate semialdehyde dehydrogenase

[a] Number of amino acids.
[b] Accession number obtained from a BLAST search.
[c] The top five significant hits from the BLAST search are shown.
[d] Number of amino acids over which the identity exists.

that $AraA_{At}$ is an arabinose, fucose, and galactose dehydrogenase (data not shown). To monitor the expression of $AraA_{At}$, an RGS-6His tag was added to the N terminus of $AraA_{At}$, and the construct was reintroduced to its original site on the chromosome to make strain AB601. This strain was used in assays to detect the expression of $AraA_{At}$ in response to different carbon sources. Western blotting showed that $AraA_{At}$ is induced by the metabolic substrates arabinose, fucose, and galactose (Fig. 9).

DISCUSSION

A. tumefaciens is a plant pathogen routinely found as a free-living saprophyte in the soil, where it is likely to encounter both deficiency of and competition for nutrients. To adapt to this environment and compete with other soilborne microorganisms, the evolution of multiple transport systems for the uptake of nutrients appears to be important as a means to acquire these nutrients, thereby obtaining energy for growth and pathogenesis. In this study, we revisited the previously characterized operon *chvE-gguABC*. Our results indicate that (i) *gguAB* is involved in transport of several different monosaccharides and (ii) *A. tumefaciens* uses a pathway to degrade L-arabinose that does not involve phosphorylated intermediates, while *gguC* encodes an enzyme in this metabolic pathway.

Tests of several different sugars—L-arabinose, D-fucose, D-galactose, D-glucose, and D-xylose—as sole carbon sources by the *gguA* and *gguB* deletion strains (AB510 and AB520, respectively) (Fig. 2) strongly supports the hypothesis that *gguAB* is involved in the import of multiple substrates. These results contrast with those of Kemner et al. (17), who reported no growth differences between the wild type and strains carrying disruptions in *gguA*, *gguB*, or *gguC*. However, our liquid growth assay is more sensitive than the colony size assay used by Kemner et al. Furthermore, Kemner et al. (17) used a sugar concentration of 1 mM, whereas our studies employed a concentration of 3 mM. The K44A mutation in GguA eliminated that protein's capacity to complement the *gguA* deletion (Fig. 4B). Given that this lysine is conserved and essential for activity in all ATP-binding proteins that are components of ABC transporters as well as the growth studies referred to above, we suggest that the current name *gguAB* be changed to *mmsAB* for multiple monosaccharide transport. The first gene in *chvE-mmsAB-gguC* operon, *chvE*, was found to be a sugar-binding protein and can bind L-arabinose, D-fucose, D-galactose, D-glucose, and D-xylose (14). Because it was first identified as a protein involved in sugar-mediated control of virulence in *A. tumefaciens*, we suggest that the *chvE* name be retained. Based on gene location and these experimental results, ChvE-MmsAB apparently constitute a complete binding-protein-dependent ABC transporter involved in the uptake of several different sugars.

The finding that the *mmsAB* deletion strains still grow, albeit slowly, in medium supplied with various sugars suggests the existence of an additional, less efficient uptake system(s) for these sugars. Many substrates are transported into the cell by multiple transport systems. For example, in *E. coli* galactose is transported by at least five systems (34). In *Agrobacterium radiobacter*, two high-affinity glucose-binding proteins (GBP1 and GBP2) were also found to bind D-galactose and D-xylose,

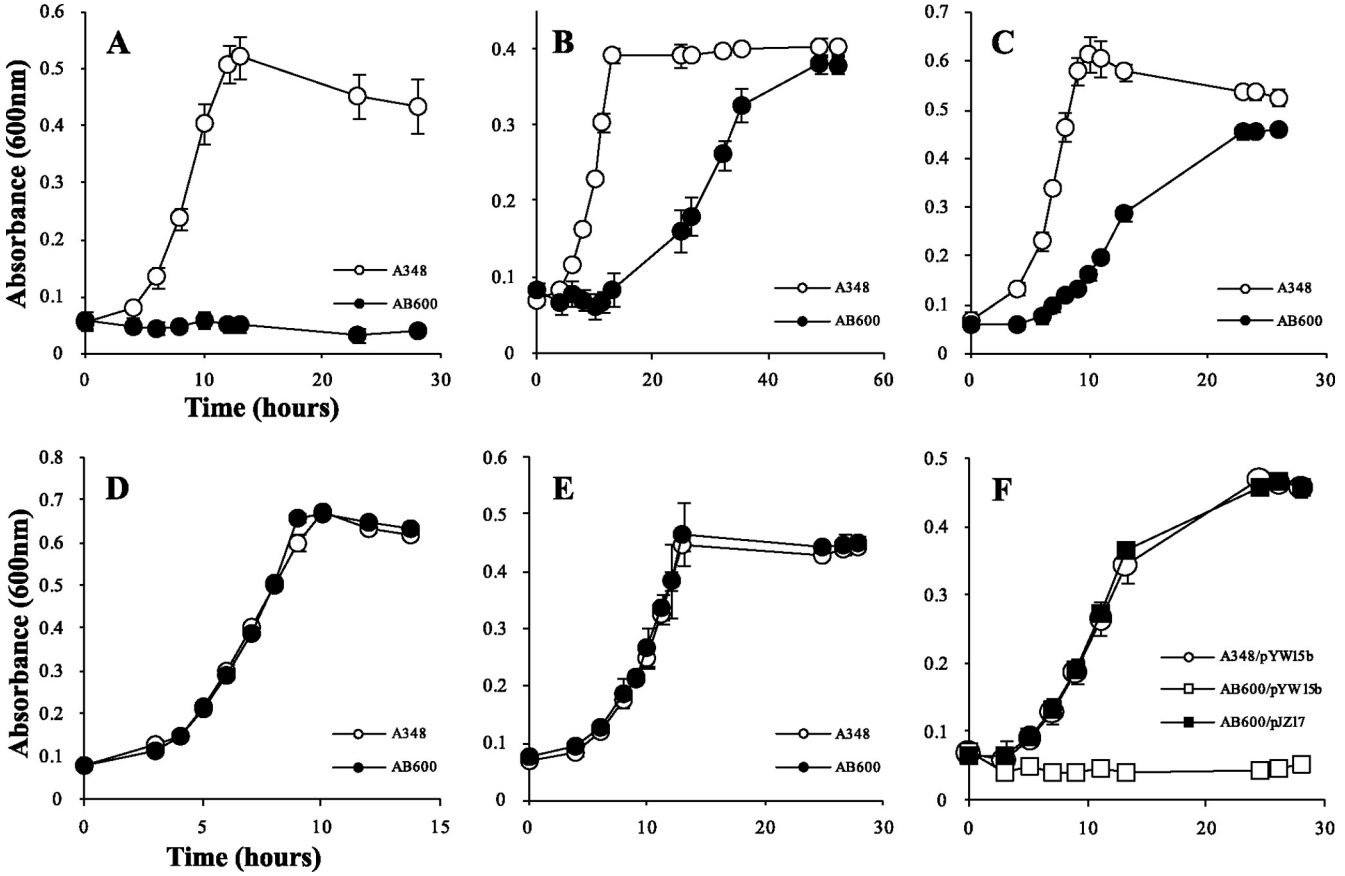

FIG. 8. Growth curves of *A. tumefaciens* wild-type strain A348 and gene locus Atu1113 deletion strain AB600 (A, B, C, D, and E) and complementation strains (F) in minimal medium containing different sugars. Bacteria were grown at 25°C in AB minimal medium with 3 mM concentrations of the monosaccharides arabinose (A and F), fucose (B), galactose (C), glucose (D), and xylose (E) as the sole carbon sources. At intervals, the optical density at 600 nm of the cultures was determined. Data are the averages of triplicate values with standard deviations.

respectively, and were involved in the transport of these sugars (6). On the basis of the amino-terminal sequence, the GBP1 and GBP2 are encoded by the gene loci Arad_3358 and Arad_3364 in the *A. radiobacter* genome (29), respectively. A BLAST search using GBP1 and GBP2 sequences against the *A. tumefaciens* genome showed that GBP1 is homologous to ChvE, while GBP2 is homologous to the protein encoded by the gene locus Atu3576. This gene locus is a part of a larger gene locus encoding transmembrane and ATP-binding proteins. We can infer that *A. tumefaciens* can also use the ABC transporter encoded by the Atu3576-related locus to transport glucose and xylose.

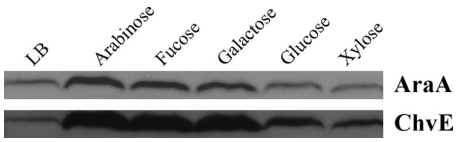

FIG. 9. Comparison of $AraA_{At}$ and ChvE expression. Strain AB601 with the RGS-His-tagged Atu1113 gene locus was grown in LB or in minimal medium containing 10 mM arabinose, fucose, galactose, glucose, or xylose as the sole carbon source. After AraA was detected with mouse anti-RGS-His antibody, the membrane was stripped and subsequently used to determine the ChvE level with rabbit anti-ChvE antibody.

In our studies, AB530 (Δ*gguC*) exhibited ligand-specific effects—growth in arabinose was vastly reduced, whereas growth in the other tested sugars was unaffected. Additionally, sequence analysis suggested that GguC has some homology to an enzyme involved in D-arabinose metabolism (see below). Two pathways for L-arabinose degradation by bacteria have been described. The first converts arabinose into a phosphorylated intermediate, while the second forms a reduced, nonphosphorylated intermediate that is subsequently metabolized. Our data indicate that *A. tumefaciens* uses the nonphosphorylation pathway to degrade L-arabinose. This pathway was recently characterized in *A. brasiliense*, and the corresponding genes have been cloned (31–33).

The enzyme activity assays with cell extracts and the growth assays with the $araA_{At}$ mutant provide strong evidence that $AraA_{At}$ is an L-arabinose dehydrogenase. Furthermore, the growth assay of AB600 ($araA_{At}$ deletion strain) indicates that $AraA_{At}$ is also involved in D-fucose and D-galactose metabolism. Consistent with the growth assays, accumulation of $AraA_{At}$ was also shown by immunoblot analysis to be stimulated by these three metabolic sugars. In *A. brasiliense*, L-

arabinose 1-dehydrogenase, encoded by *araA*, was also shown to oxidize other sugars, such as D-galactose and D-xylose, *in vitro*. In contrast to $araA_{At}$ in *A. tumefaciens*, the expression of *araA* in *A. brasiliense* was found to be induced only by L-arabinose, and a strain with an *araA* disruption exhibited a growth defect only in a minimal medium with L-arabinose as the sole carbon source. Thus, it appears that $araA_{At}$ has novel and substantial roles in the metabolism of at least arabinose, galactose, and fucose.

The enzymatic activity encoded by *gguC* remains unresolved. One clue concerning its possible activity comes from the characterization of the metabolic pathway for D-arabinose, the C4 epimer of L-arabinose in *Sulfolobus solfataricus*, a member of the *Archaea* (2). KdaD (2-keto-3-deoxy-D-arabinonate dehydratase) catalyzes the dehydration step from 2-keto-3-deoxy-D-arabinonate (D-KDA). Interestingly, GguC has some homology to KdaD (expect value, 2e-17; 34% identity over 184 residues), and both proteins have a fumarylacetoacetate hydrolase domain in their C termini. Based on sequence alignment, most of the active sites for metal and substrate binding were found in GguC (data not shown). We propose that GguC is functionally homologous to KdaD but uses L-KDA as the substrate (Fig. 7). An important observation, however, is that while a deletion of $araA_{At}$ completely eliminates growth in L-arabinose, the deletion of *gguC* only slows growth in this sugar, suggesting redundancy in the pathway. One candidate for a second KdaD was revealed by a BLAST search. We found that the protein encoded at gene locus Atu5457 in *A. tumefaciens* is a homolog to AraD (expect value, 2e-20; 31% identity over 286 residues) (Table 3), the gene product 2-keto-3-deoxy-L-arabinonate dehydratase involved in catabolism of L-arabinose in *A. brasiliense* (33), and may have a similar function. Given the growth-defective phenotype of the *gguC* mutant (AB530) in arabinose medium, we hypothesize that *A. tumefaciens* uses two distinct but functionally similar enzymes to break down 2-keto-3-deoxy-L-arabinonate. To follow the nomenclature for 2-keto-3-deoxy-L-arabinonate dehydratase in *A. brasiliense*, we propose renaming *gguC* as *araD1* and gene locus Atu5457 as *araD2*.

Biochemical studies have revealed that *Sinorhizobium meliloti* uses the same pathway as *A. brasiliense* to metabolize L-arabinose (12). Recently, by mutagenesis, the gene cluster *araABCDEF* was found to be necessary for L-arabinose utilization (24). Among this gene cluster, *araABCD* were homologous to *chvE-mmsAB-araD1*. While L-arabinose dehydrogenase activity was found in this strain, the gene for that enzyme has not yet been identified. Based on our BLAST search, we found that the gene product of SMc00588 has significant homology to $AraA_{At}$ (expect value, 5e-140; 58% identity over 308 residues), making it a good candidate for L-arabinose dehydrogenase.

In conclusion, this study provides the first evidence for a pathway lacking phosphorylated intermediates to degrade L-arabinose in *A. tumefaciens*. Further study is still needed to elucidate the entire pathway for L-arabinose metabolism. Finally, our results suggest that L-arabinose is one of the substrates transported by the binding-protein-dependent ABC transport system ChvEMmsAB, which also transports D-fucose, D-galactose, D-glucose, and D-xylose.

ACKNOWLEDGMENTS

We thank Arlene A. Wise for critically reading an earlier version of the manuscript. We thank Erik Ronzone for the initial BLAST analysis indicating that GguC is homologous to KdaD of *Sulfolobus solfataricus*.

This work was partially funded by grant 0818613 from the National Science Foundation.

REFERENCES

1. **Alvarez-Martinez, M. T., et al.** 2001. The *Brucella suis* homologue of the *Agrobacterium tumefaciens* chromosomal virulence operon *chvE* is essential for sugar utilization but not for survival in macrophages. J. Bacteriol. **183:** 5343–5351.
2. **Brouns, S. J., et al.** 2006. Identification of the missing links in prokaryotic pentose oxidation pathways: evidence for enzyme recruitment. J. Biol. Chem. **281:**27378–27388.
3. **Camacho, L. R., D. Ensergueix, E. Perez, B. Gicquel, and C. Guilhot.** 1999. Identification of a virulence gene cluster of *Mycobacterium tuberculosis* by signature-tagged transposon mutagenesis. Mol. Microbiol. **34:**257–267.
4. **Cheng, J., A. A. Guffanti, and T. A. Krulwich.** 1997. A two-gene ABC-type transport system that extrudes Na^+ in *Bacillus subtilis* is induced by ethanol or protonophore. Mol. Microbiol. **23:**1107–1120.
5. **Chilton, M. D., et al.** 1974. *Agrobacterium tumefaciens* DNA and PS8 bacteriophage DNA not detected in crown gall tumors. Proc. Natl. Acad. Sci. U. S. A. **71:**3672–3676.
6. **Cornish, A., J. A. Greenwood, and C. W. Jones.** 1989. Binding-protein-dependent sugar transport by *Agrobacterium radiobacter* and *A. tumefaciens* grown in continuous culture. J. Gen. Microbiol. **135:**3001–3013.
7. **Cribbs, R., and E. Englesberg.** 1964. L-arabinose negative mutants of the L-ribulokinase structural gene affecting the levels of L-arabinose isomerase in *Escherichia coli*. Genetics **49:**95–108.
8. **Decleene, M., and J. Deley.** 1976. Host range of crown gall. Bot. Rev. **42:**389–466.
9. **Deyrup, A. T., S. Krishnan, B. N. Cockburn, and N. B. Schwartz.** 1998. Deletion and site-directed mutagenesis of the ATP-binding motif (P-loop) in the bifunctional murine ATP-sulfurylase/adenosine 5′-phosphosulfate kinase enzyme. J. Biol. Chem. **273:**9450–9456.
10. **Dische, Z., and E. Borenfreund.** 1951. A new spectrophotometric method for the detection and determination of keto sugars and trioses. J. Biol. Chem. **192:**583–587.
11. **Doty, S. L., M. Chang, and E. W. Nester.** 1993. The chromosomal virulence gene, *chvE*, of *Agrobacterium tumefaciens* is regulated by a LysR family member. J. Bacteriol. **175:**7880–7886.
12. **Duncan, M. J.** 1979. L-arabinose metabolism in rhizobia. J. Gen. Microbiol. **113:**177–179.
13. **Garfinkel, D. J., and E. W. Nester.** 1980. *Agrobacterium tumefaciens* mutants affected in crown gall tumorigenesis and octopine catabolism. J. Bacteriol. **144:**732–743.
14. **He, F., et al.** 2009. Molecular basis of ChvE function in sugar binding, sugar utilization, and virulence in *Agrobacterium tumefaciens*. J. Bacteriol. **191:** 5802–5813.
15. **Higgins, C. F.** 1992. ABC transporters: from microorganisms to man. Annu. Rev. Cell Biol. **8:**67–113.
16. **Higuchi, R., B. Krummel, and R. K. Saiki.** 1988. A general method of in vitro preparation and specific mutagenesis of DNA fragments: study of protein and DNA interactions. Nucleic Acids Res. **16:**7351–7367.
17. **Kemner, J. M., X. Liang, and E. W. Nester.** 1997. The *Agrobacterium tumefaciens* virulence gene *chvE* is part of a putative ABC-type sugar transport operon. J. Bacteriol. **179:**2452–2458.
18. **Kovach, M. E., et al.** 1995. Four new derivatives of the broad-host-range cloning vector pBBR1MCS, carrying different antibiotic-resistance cassettes. Gene **166:**175–176.
19. **Laemmli, U. K.** 1970. Cleavage of structural proteins during the assembly of the head of bacteriophage T4. Nature **227:**680–685.
20. **Linton, K. J., and C. F. Higgins.** 1998. The *Escherichia coli* ATP-binding cassette (ABC) proteins. Mol. Microbiol. **28:**5–13.
21. **McCullen, C. A., and A. N. Binns.** 2006. *Agrobacterium tumefaciens* and plant cell interactions and activities required for interkingdom macromolecular transfer. Annu. Rev. Cell Dev. Biol. **22:**101–127.
22. **Miller, J. H.** 1972. Experiments in molecular genetics. Cold Spring Harbor Laboratory, Cold Spring Harbor, NY.
23. **Neidhardt, F. C.** 1987. *Escherichia coli* and *Salmonella typhimurium*: cellular and molecular biology. American Society for Microbiology, Washington, DC.
24. **Poysti, N. J., E. D. Loewen, Z. Wang, and I. J. Oresnik.** 2007. *Sinorhizobium meliloti* pSymB carries genes necessary for arabinose transport and catabolism. Microbiology **153:**727–736.
25. **Pradhan, P., W. Li, and P. Kaur.** 2009. Translational coupling controls expression and function of the DrrAB drug efflux pump. J. Mol. Biol. **385:** 831–842.

26. **Rees, D. C., E. Johnson, and O. Lewinson.** 2009. ABC transporters: the power to change. Nat. Rev. Mol. Cell Biol. **10:**218–227.
27. **Schafer, A., et al.** 1994. Small mobilizable multi-purpose cloning vectors derived from the *Escherichia coli* plasmids pK18 and pK19: selection of defined deletions in the chromosome of *Corynebacterium glutamicum*. Gene **145:**69–73.
28. **Schneider, E.** 2001. ABC transporters catalyzing carbohydrate uptake. Res. Microbiol. **152:**303–310.
29. **Slater, S. C., et al.** 2009. Genome sequences of three *Agrobacterium* biovars help elucidate the evolution of multichromosome genomes in bacteria. J. Bacteriol. **191:**2501–2511.
30. **Wang, Y., A. Mukhopadhyay, V. R. Howitz, A. N. Binns, and D. G. Lynn.** 2000. Construction of an efficient expression system for *Agrobacterium tumefaciens* based on the coliphage T5 promoter. Gene **242:**105–114.
31. **Watanabe, S., T. Kodaki, and K. Makino.** 2006. Cloning, expression, and characterization of bacterial L-arabinose 1-dehydrogenase involved in an alternative pathway of L-arabinose metabolism. J. Biol. Chem. **281:**2612–2623.
32. **Watanabe, S., T. Kodaki, and K. Makino.** 2006. A novel alpha-ketoglutaric semialdehyde dehydrogenase: evolutionary insight into an alternative pathway of bacterial L-arabinose metabolism. J. Biol. Chem. **281:** 28876–28888.
33. **Watanabe, S., N. Shimada, K. Tajima, T. Kodaki, and K. Makino.** 2006. Identification and characterization of L-arabonate dehydratase, L-2-keto-3-deoxyarabonate dehydratase, and L-arabinolactonase involved in an alternative pathway of L-arabinose metabolism. Novel evolutionary insight into sugar metabolism. J. Biol. Chem. **281:**33521–33536.
34. **Wilson, D. B.** 1978. Cellular transport mechanisms. Annu. Rev. Biochem. **47:**933–965.
35. **Wood, D. W., et al.** 2001. The genome of the natural genetic engineer *Agrobacterium tumefaciens* C58. Science **294:**2317–2323.